Structural Engineering and Mechanics, Vol. 43, No. 6 (2012) 739-759
DOI: http://dx.doi.org/10.12989/sem.2012.43.6.739

Extension of a new tailoring optimisation technique to sandwich shells with laminated faces

Ugo Icardi*

Dipartimento di Ingegneria Meccanica e Aerospaziale,
Politecnico di Torino - Corso Duca degli Abruzzi 24, 10129 Torino, Italy

(Received March 28, 2011, Revised May 15, 2012, Accepted August 7, 2012)

Abstract. The tailoring optimization technique recently developed by the author for improving structural response and energy absorption of composites is extended to sandwich shells using a previously developed zig-zag shell model with hierarchic representation of displacements. The in-plane variation of the stiffness properties of plies and the through-the thickness variation of the core properties are determined solving the Euler-Lagrange equations of an extremal problem in which the strain energy due to out-of-plane strains and stresses is minimised, while that due to their in-plane counterparts is maximised. In this way, the energy stored by unwanted out-of-plane modes involving weak properties is transferred to acceptable in-plane modes. As shown by the numerical applications, the critical interlaminar stress concentrations at the interfaces with the core are consistently reduced without any bending stiffness loss and the strength to debonding of faces from the core is improved. The structural model was recently developed by the author to accurately describe strain energy and interlaminar stresses from the constitutive equations. It *a priori* fulfills the displacement and stress contact conditions at the interfaces, considers a second order expansion of Lame's coefficients and a hierarchic representation that adapts to the variation of solutions. Its functional d.o.f. are the traditional mid-plane displacements and the shear rotations, so refinement implies no increase of the number of functional d.o.f. Sandwich shells are represented as multilayered shells made of layers with different thickness and material properties, the core being treated as a thick intermediate layer.

Keywords: tailoring optimisation; stress relaxation; strength improvement; sandwich shell; zig-zag model

1. Introduction

Sandwich composites with laminated faces are extensively employed owing to their low weigh, high bending stiffness, superior energy absorption, thermal and sound insulation characteristics and good behaviour under fatigue.

Shear key (see, Mitra 2010), insertion of fibres through the thickness by a tufting process (see, Henao *et al*. 2010) or interlocks (Younes and Zaki 2011) may be used for improving the structural performance, interlaminar strength and damage tolerance of these materials. Stitching, special lap and *T* joints, may also be employed for preventing interlaminar stress concentrations and to oppose

*Corresponding author, Professor, E-mail: ugo.icardi@polito.it

the propagation of delamination in the faces.

Because the face layers have directional properties that can be tailored, traditionally the structural performance of sandwiches is optimised by finding the appropriate ply angles and stacking sequence that maximise design requirements. As examples of ply angles optimization studies and of sandwich optimization, the papers by Chaperon *et al*. (2000), Hudson *et al*. 2010, Jones *et al*. (2000), Keller (2010), Kaye and Heller (2000), Sivakumar *et al*. (2000) are cited. Customary, finite element or closed form analytic approaches are used to evaluate objective function and constraints. Gradient based search techniques or genetic algorithms (see, e.g., Uys *et al*. 2003, Krishnapillai and Jones 2009, respectively) are employed to efficiently solve the optimal lamination problem. The structural response is generally computed using smeared laminate models, the computational effort of more realistic models being unaffordable for the optimisation process. Thus, the layerwise effects that adversely affect strength, stiffness, failure behaviour and service life of composites may not be accurately predicted.

As the fibre orientation angle is considered constant throughout the plies and the core properties are assumed uniform across the thickness, an excellent opportunity for improving performance and damage tolerance of sandwiches and for enlarging their life in service may not be fully exploited. In particular, the interlaminar stress concentration due to the different mechanical properties of faces and core may not be recovered with constant stiffness properties. Hence, debonding can lead to stiffness loss, bending and buckling failure in service.

Variable-stiffness composites in which the fibres follow curvilinear paths in order the properties can be varied at each point to meet design requirements have been considered since two decades (see, Hyer and Charette 1991, Heyer and Lee 1991). This tailoring option has been recently retaken (Ghiasi *et al*. 2010, Javidrad and Nouri 2011) as it offers advantages over straight-fibre laminates like the improvement of buckling and first-ply failure loads (Jegley *et al*. 2005, Lopes *et al*. 2008), the maximisation of stiffness (Pedersen 2003, Setoodeh *et al*. 2005) and an increase of the fundamental frequency (Diaconu *et al*. 2002, Narita and Hodgkinson 2005, Abdalla *et al*. 2007). Jung (2001), Lakes (2002) proven that structural hierarchy guided combinations of materials with different stiffness/dissipation properties make possible the obtainment of desired structural properties without any stiffness loss. The advent of variable stiffness composites is allowed by new technologies such automated fibre-placement (Barth 1990, Enders and Hopkins 1991, Martin *et al*. 1997, Evans 2001) and functionally graded materials (FGM) (see, e.g., Fuchiyama and Noda 1995, Suresh and Mortensen 1998, Mahfuz *et al*. 2004). Recent studies on FGM by Sankar (2001), Sankar and Tzeng (2002), Venkataraman and Sankar (2001), Apetre *et al*. (2002, 2003, 2006), Zhu and Sankar (2004), Reid and Paskaramoorthy (2011) have proven the great potential advantages of variable-stiffness materials.

Variable-stiffness sandwiches with the properties of faces and core that vary at each point may offer a good chance for meeting an enlarged set of design requirements and other important advantages, because the concentration of interlaminar stresses at interfacial material discontinuities can be fully recovered. But the possibility of varying the strength and stiffness properties at each point comes at the price of a significantly enlarged number of design variables. As a consequence, the traditional optimization techniques based on gradient search or genetic algorithms may become computationally too expensive with variable-stiffness composites, making unpractical these materials. An advanced optimization technique based on the modified particle swarm approach has been developed by Sepehri *et al*. (2012) that overcomes the problem.

A tailoring optimisation technique based on variable-stiffness concepts (OPTI) has been recently

developed by Icardi and Ferrero (2008, 2009a, b, 2010) that provides the fibre angle variation of the face plies and the through-thickness distribution of the core properties by solving the Euler-Lagrange equations that follows by setting the first variation of the strain energy to zero under spatial variation of the stiffness properties.

As the optimal spatial distribution of the stiffness properties is computed solving the Euler-Lagrange equations, the optimisation problem of variable-stiffness composites turns into the more simple problem of finding the appropriate stacking sequence like with straight-fibre composites, which can be efficiently solved using classical optimisation techniques.

OPTI was developed with the purpose of minimising the energy stored by the modes involving large out-of-plane strains and stresses and maximising that of modes with dominant membrane strains and stresses, since laminated and sandwich composites have a much smaller strength and stiffness in the thickness direction than in the in-plane direction. In Icardi and Ferrero (2008), applications were presented to laminated plates subject to low velocity, low energy impacts, which proven that beneficial effects may be obtained on the strength at the onset of delamination incorporating layers with spatially variable optimised properties. In Icardi and Ferrero (2009a), sandwich flat panels with through-the-thickness variable distributions of the core properties and variable in-plane distributions of the face plies properties were considered under blast pulse loading, to show that wanted dynamic response properties can be achieved recovering the critical interlaminar stresses. In Icardi and Ferrero (2009b), the optimisation of sandwich flat panels were carried out using a finite element scheme based on strain energy updating concepts. In Icardi and Ferrero (2010), an improved "tuning" capability of double-core sandwich flat panels over single core sandwiches was shown. In these studies, a 3D zig-zag plate model with a third-order piecewise variation of the in-plane displacements and a fourth-order piecewise variation of the transverse displacement across the thickness which *a priori* fulfil the interlaminar stress contact conditions at the interfaces was employed as structural model (Icardi 2001).

In the present paper, OPTI is extended to curved single and double-core sandwich panels. Because the core properties are still varied within the range of available foams by stacking the stiffer materials close to the faces and the weaker ones at the mid-plane, a layerwise model should be used as structural model to capture the non-planar deformations and stresses that still rise at the interfaces. So, on the contrary of the studies on FGM, the effects of interfacial material discontinuities should still be accounted for. The goal is finding the spatial variation of stiffness properties of faces and core of sandwich shells that minimise the energy due to interlaminar stresses and maximises the bending stiffness as, without an enhanced interfacial bond strength, the coupling between in-plane and out-of-plane deformations due to curvatures may result in performance loss and premature failure in service.

Here the multi-layered 3D zig-zag shell model by Icardi and Ferrero (2011) with a hierarchic representation of the displacements across the thickness is employed, because it accurately describes the strain energy. The classical mid-plane displacements and shear rotations are assumed as functional d.o.f. to have the minimal number of primary variables. The displacement fields are constructed as the sum of polynomials with continuous gradients across the thickness, piecewise continuous functions that makes discontinuous the gradients at the interfaces and higher-order adaptive terms. The model was constructed to provide accurate stress predictions by the constitutive equations, because integration of local differential equations may not provide accurate interlaminar stresses, as shown by Cho *et al*. (1996), Li and Liu (1997), Zhen and Wanji (2008).

The paper is structured as follows. The features of the structural shell model and the basic steps

towards its development are a briefly discussed. Next the process for deriving the Euler-Lagrange equations which represent the stationary conditions under variation of the stiffness properties is reviewed, to show how the contributions of curvatures and hierarchic terms make the optimisation problem different from that of the previous studies. Afterwards numerical applications are presented to single and double-core sandwiches with laminated faces in cylindrical bending.

2. Structural model

To sum up, the multi-layered structural models for analysis of laminated and sandwich composites can have a variable or a fixed number of functional d.o.f. In the former case, they can be refined across the thickness and a different representation can be used in different regions, but a large computational effort is required, thus they should be limited to local analyses for not overwhelming the computational capacity. Those with a fixed number of functional d.o.f. cannot be refined across the thickness, so they have a limited validity for stress analysis. However, they can be accurate if post-processing techniques may be employed for refining the stress predictions.

The model based on a hierarchic representation used in the present paper accurately describes the strain energy storage and the interlaminar stresses with a low computational effort. The following piecewise representation of the displacements is postulated across the thickness (Icardi and Ferrero 2011)

$$u_\alpha(\alpha,\beta,\zeta) = \left(1+\frac{\zeta}{R_\alpha}\right)u_\alpha^{(0)}(\alpha,\beta) - \zeta\frac{u_{\zeta,\alpha}^{(0)}(\alpha,\beta)}{A_\alpha} + \zeta(1+(C_{2\alpha}(\alpha,\beta)\zeta + C_{3\alpha}(\alpha,\beta)\zeta^2))\gamma_\alpha^{(0)}(\alpha,\beta) + (O\zeta^4\ldots) + \sum_{k=1}^{S}\Phi_\alpha^{(k)}(\alpha,\beta)(\zeta-\zeta^{(k)})\mathscr{H}_{.k} \tag{1}$$

$$u_\beta(\alpha,\beta,\zeta) = \left(1+\frac{\zeta}{R_\beta}\right)u_\beta^{(0)}(\alpha,\beta) - \zeta\frac{u_{\zeta,\beta}^{(0)}(\alpha,\beta)}{A_\beta} + \zeta(1+(C_{2\beta}(\alpha,\beta)\zeta + C_{3\beta}(\alpha,\beta)\zeta^2))\gamma_\beta^{(0)}(\alpha,\beta) + (O\zeta^4\ldots) + \sum_{k=1}^{S}\Phi_\beta^{(k)}(\alpha,\beta)(\zeta-\zeta^{(k)})\mathscr{H}_{.k} \tag{2}$$

$$u_\zeta(\alpha,\beta,\zeta) = a(\alpha,\beta) + \zeta b(\alpha,\beta) + \zeta^2 c(\alpha,\beta) + \zeta^3 d(\alpha,\beta) + \zeta^4 e(\alpha,\beta) + (O\zeta^5\ldots) + \sum_{k=1}^{S-1}\Psi_\zeta^{(k)}(\alpha,\beta)(\zeta-{}^{(k)}\zeta)\mathscr{H}_k + \sum_{k=1}^{S-1}\Omega_\zeta^{(k)}(\alpha,\beta)(\zeta-{}^{(k)}\zeta^2)\mathscr{H}_k \tag{3}$$

which can be refined across the thickness without increasing the number of primary variables suitably choosing the contributions $(O\zeta^4\ldots)$ and $(O\zeta^5\ldots)$, as outlined hereafter. The three components of the elastic displacement in the direction of the axes α, β and ζ are indicated as u_α, u_β, respectively. The curvilinear tri-orthogonal system constituted by the lines α, β of principal curvature and by the coordinate across the thickness ζ is assumed as reference system. The symbols $R_\alpha(\alpha,\beta)$ and $R_\beta(\alpha,\beta)$ represent the radii, $(\,)_{,\alpha}, (\,)_{,\beta}$ denote differentiation with respect to the spatial ordinates, while the quantities related to a generic layer k are denoted with a suffix$^{(k)}$. The

Lamé coefficients are indicated with $A_\alpha(\alpha,\beta)$, $A_\beta(\alpha,\beta)$; their reciprocals $1/H_\alpha$, $1/H_\beta$ are expanded up to the second order across the thickness.

The terms in the summations are the zig-zag contributions whose purpose is to make discontinuous the derivatives of displacements at the layer interfaces for *a priori* fulfilling the continuity of transverse shear and normal stresses and of the transverse normal stress gradient, as prescribed by the elasticity theory for keeping equilibrium. $\mathscr{H}_{.k}$ is the Heaviside unit step function ($\mathscr{H}_{.k} = \mathscr{H}_{.k}(\zeta-\zeta^{(k)}) = 1$ for $\zeta \geq \zeta^{(k)}$ and 0 for $\zeta < \zeta^{(k)}$) which enables the fulfillment of such stress contact conditions with a suited choice of the continuity functions $\Phi_\alpha^{(k)}, \Phi_\beta^{(k)}, \Psi_\zeta^{(k)}, \Omega_\zeta^{(k)}$. The three displacements $u_\alpha^{(0)}, u_\beta^{(0)}, u_\zeta^{(0)}$ and the two shear rotations $\gamma_\alpha^{(0)}, \gamma_\beta^{(0)}$ of the points on the reference middle surface of the shell represent the functional d.o.f. The meaning of the other symbols is as follows. $C_{2\alpha}, C_{3\alpha}, C_{2\beta}, C_{3\beta}$ represent coefficients whose expressions in terms of the functional d.o.f. and their derivatives are determined by enforcing the fulfilment of the stress-free boundary conditions on transverse shear stresses at the upper and lower bounding faces. The symbol a plays as the transverse displacement on the reference mid-plane $u_\zeta^{(0)}$, while the coefficients b to e are determined by enforcing the boundary conditions on the transverse normal stress and its gradient at the upper and lower bounding surfaces.

The expressions of the continuity functions $\Phi_\alpha^{(k)}, \Phi_\beta^{(k)}, \Psi_\zeta^{(k)}, \Omega_\zeta^{(k)}$ in terms of the d.o.f. and of their derivatives are determined in a straightforward way by enforcing the continuity of the interlaminar transverse shear and normal stresses and of the transverse normal stress gradient at the layer interfaces. These expressions are here omitted as they are shown in the paper by Icardi and Ferrero (2011).

The higher-order terms $(O\zeta^4\ldots)$ and $(O\zeta^5\ldots)$ represent the hierarchic part of the representation that can adapt to the problem, allowing a refinement across the thickness. They give contributions of the following form

$$P_J^n(\mathscr{H}_{n-1} - \mathscr{H}_n) + P_J^m(\mathscr{H}_{m-1} - \mathscr{H}_m) + \ldots \tag{4}$$

P_J^n and P_J^m being polynomials whose expressions are

$$P_\alpha^\upsilon = A^\alpha\zeta^4 + B^\alpha\zeta^5 + C^\alpha\zeta^6 + D^\alpha\zeta^7 + E^\alpha\zeta^8 + \ldots \tag{5}$$

$$P_\beta^\nu = A^\beta\zeta^4 + B^\beta\zeta^5 + C^\beta\zeta^6 + D^\beta\zeta^7 + E^\beta\zeta^8 + \ldots \tag{6}$$

$$P_\zeta^\nu = A^\zeta\zeta^5 + B^\zeta\zeta^6 + C^\zeta\zeta^7 + D^\zeta\zeta^8 + E^\zeta\zeta^9 + \ldots \tag{7}$$

the symbol ν being used for representing n and m, whereas $P_\alpha^\upsilon, P_\beta^\nu$ and P_ζ^ν represent the contributions incorporated in u_α, u_β and u_ζ, respectively. The coefficients of the higher-order powers $A^\alpha\ldots E^\alpha$, $A^\beta\ldots E^\beta, A^\zeta\ldots E^\zeta$ are determined in a straightforward way by enforcing equilibrium conditions at selected points across the thickness.

The stress continuity conditions should be restored at the points across the thickness where the representation by re-computing the expressions of the continuity functions $\Phi_\alpha^{(k)}, \Phi_\beta^{(k)}, \Psi_\zeta^{(k)}, \Omega_\zeta^{(k)}$, as the material properties do not change, but the interlaminar stresses are discontinuous since the expression of displacements have been changed. The derivation of governing equations is omitted, since they are obtained with the standard techniques (e.g., the principle of virtual work, or the total potential energy principle) substituting the previous expressions.

3. Optimisation of the energy storage

The purpose of the strain energy optimisation process is finding a suited distribution of the stiffness properties that minimises the energy absorbed through undesired modes (e.g., modes involving interlaminar strengths) and maximises that absorbed by desired modes (e.g., modes involving membrane strengths). This distribution is determined by solving the Euler-Lagrange equations that are obtained by making extremal the in-plane, bending and out-of-plane shear contributions to strain energy under spatial variation of the stiffness properties.

The effect of this technique is to act as an energy "*tuning*", since the amount of the energy stored by specific modes can be minimised, or maximised, as desired, with a suited distribution of the stiffness properties.

3.1 Stationary conditions for the strain energy

First, the expressions of the strains are obtained from the displacements fields using linear strain-displacement relations (Icardi and Ferrero 2011)

$$\varepsilon_{\alpha\alpha} = \frac{u_{\alpha,\alpha}}{H_\alpha} + \frac{H_{\alpha,\beta}}{H_\alpha H_\beta} u_\beta + \frac{H_{\alpha,\zeta}}{H_\alpha H_\zeta} u_\zeta \tag{8}$$

$$\varepsilon_{\beta\beta} = \frac{u_{\beta,\beta}}{H_\beta} + \frac{H_{\beta,\alpha}}{H_\alpha H_\beta} u_\alpha + \frac{H_{\beta,\zeta}}{H_\beta H_\zeta} u_\zeta \tag{9}$$

$$\varepsilon_{\alpha\beta} = \frac{H_\alpha}{H_\beta}\left(\frac{u_\alpha}{H_\alpha}\right)_{,\beta} + \frac{H_\beta}{H_\alpha}\left(\frac{u_\beta}{H_\beta}\right)_{,\alpha} \tag{10}$$

$$\varepsilon_{\alpha\zeta} = \frac{H_\alpha}{H_\zeta}\left(\frac{u_\alpha}{H_\alpha}\right)_{,\zeta} + \frac{H_\zeta}{H_\alpha}\left(\frac{u_\zeta}{H_\zeta}\right)_{,\alpha} \tag{11}$$

$$\varepsilon_{\beta\zeta} = \frac{H_\beta}{H_\zeta}\left(\frac{u_\beta}{H_\beta}\right)_{,\zeta} + \frac{H_\zeta}{H_\beta}\left(\frac{u_\zeta}{H_\zeta}\right)_{,\beta} \tag{12}$$

$$\varepsilon_{\varsigma\varsigma} = \frac{1}{H_\varsigma} u_{\varsigma,\varsigma} \tag{13}$$

with $1/H_\alpha$, $1/H_\beta$ approximated up to the second-order ($H_\zeta = 1$)

$$\frac{1}{H_\alpha} = \frac{1}{A_\alpha}\left(1 - \frac{\zeta}{R_\alpha} + \left(\frac{\zeta}{R_\alpha}\right)^2\right) \tag{14}$$

$$\frac{1}{H_\beta} = \frac{1}{A_\beta}\left(1 - \frac{\zeta}{R_\beta} + \left(\frac{\zeta}{R_\beta}\right)^2\right) \tag{15}$$

then the stresses are written using the stress-strain relations. Work-conjugating the stresses and the strains, the strain energy of the shell model is written. It could be noticed that the expressions of continuity functions and hierarchic contributions involve derivatives of the functional d.o.f. up to the third order with respect to the spatial coordinates α, β, ζ, thus high order derivatives of

displacements are involved, which can be recovered as outlined in Icardi and Ferrero (2011) in order to develop finite elements.

- The procedure starts by enforcing the vanishing of the first variation of the strain energy under variation of the functional d.o.f., which associated to the variation of the external work represents the equilibrium condition.
- The strain energy is made of terms which are obtained by integrating in ζ the product of elastic coefficients and powers of ζ of various orders representing the stiffness coefficients of the model, and in-plane derivatives of the functional d.o.f.
- The optimised distributions are obtained solving the Euler-Lagrange equations which follows by enforcing the vanishing of the first variation of the strain energy under variation of the stiffness properties. These stationary conditions are obtained integrating by parts the derivatives of the functional d.o.f. $u_\alpha^{(0)}, u_\beta^{(0)}, u_\zeta^{(0)}, \gamma_\alpha^{(0)}, \gamma_\beta^{(0)}$ that appear in the expression of the first variation of the strain energy with respect to the displacements d.o.f.
- According, the derivatives of the functional d.o.f. turn into derivatives of the same order of the stiffness coefficients. The final form of the equations representing the extremal conditions under in-plane variation of the stiffness properties, which hold irrespective for the displacements, are obtained collecting apart all the stiffness contributions that multiply any single d.o.f.
- The contribution by the terms that multiply $u_\zeta^{(0)}$ is referred as the strain energy in bending, those which multiply $\gamma_\alpha^{(0)}, \gamma_\beta^{(0)}$ as the strain energy of transverse shears. The tailoring optimization consists in finding stiffness distributions that simultaneously solve these equations. The in-plane contributions multiplying $u_\alpha^{(0)}, u_\beta^{(0)}$ are disregarded because laminated and sandwich composites have a larger strength and stiffness in the in-plane direction than in the thickness direction.
- The tailoring optimisation process should be split into tailoring of the face plies, which is carried out in α, β, and tailoring of the core, which is carried out in ζ, as they requires a different treatment.

3.2 Tailoring of the face plies

The following stationary condition for the bending energy

$$(WR_{11}^{\alpha} + \ldots + WR_{1i}^{\alpha})\delta u_\alpha^{(0)} + (WR_{21}^{\beta} + \ldots + WR_{2j}^{\beta})\delta u_\beta^{(0)} + (WR_{31}^{\zeta} + \ldots + WR_{3k}^{\zeta})\delta u_\zeta^{(0)} +$$
$$(WR_{41}^{\gamma\alpha} + \ldots + WR_{4m}^{\gamma\alpha})\delta\gamma_\alpha^{(0)} + (WR_{51}^{\gamma\beta} + \ldots + WR_{5n}^{\gamma\beta})\delta\gamma_\beta^{(0)} = 0 \tag{16}$$

is obtained integrating by parts the virtual variation of the strain energy under variation of the functional d.o.f. and collecting the contributions that multiply each displacement d.o.f.

The stationary condition for the transverse shear energy in the plane (α, ζ) is obtained with the same procedure as

$$(XR_{R1}^{\alpha} + \ldots + XR_{Ri}^{\alpha})\delta u_\alpha^{(0)} + (XR_{R2}^{\beta} + \ldots + XR_{Rj}^{\beta})\delta u_\beta^{(0)} + (XR_{R3}^{\zeta} + \ldots + XR_{Rk}^{\zeta})\delta u_\zeta^{(0)} +$$
$$(XR_{R4}^{\gamma\alpha} + \ldots + XR_{Rm}^{\gamma\alpha})\delta\gamma_\alpha^{(0)} + (XR_{R5}^{\gamma\beta} + \ldots + XR_{Rn}^{\gamma\beta})\delta\gamma_\beta^{(0)} = 0 \tag{17}$$

They represent partial differential equations since the terms $WR_{11}^{\alpha} \ldots WR_{5n}^{\gamma\beta}$, $WR_{R1}^{\alpha} \ldots WR_{Rn}^{\gamma\beta}$ are spatial derivatives of the stiffness properties obtained after integration by parts of the derivatives of

the displacement d.o.f., whose explicit form is discussed hereafter. Similar equations yield for the strain energy contribution in the plane (β,ζ) and for the membrane contributions but, as mentioned above, just those involving bending and transverse shear energy are here considered because laminated and sandwich composites have weak out-of-plane properties and strong in-plane properties. Thus, just the contributions under brackets that multiply $\delta u_{\zeta}^{(0)}, \delta\gamma_{\alpha}^{(0)}, \delta\gamma_{\beta}^{(0)}$ require a simultaneous solution. As the extremal condition under variation of the stiffness properties yields irrespective of the response, Eqs. (16) and (17) split into a set of partial differential equations of the following form

$$(WR_{31}^{\zeta}+\ldots+WR_{3k}^{\zeta})=0;\ (WR_{41}^{\gamma\alpha}+\ldots+WR_{4m}^{\gamma\alpha})=0;\quad (WR_{51}^{\gamma\beta}+\ldots+WR_{5n}^{\gamma\beta})=0 \tag{16'}$$

$$\{WR_{R3}^{\zeta}+\ldots+WR_{Rk}^{\zeta}\}=0;\ \{WR_{R4}^{\gamma\alpha}+\ldots+WR_{Rm}^{\gamma\alpha}\}=0;\ \{WR_{R5}^{\gamma\beta}+\ldots+WR_{Rn}^{\gamma\beta}\}=0 \tag{17'}$$

whose simultaneous solution provides the distribution of the spatial stiffness properties that make extremal the bending and transverse shear energy contributions. The corresponding distribution of the elastic coefficients $Q_{ij}=Q_{ij}(\alpha,\beta)$ (ij = 11, 12, 13, 22, 23, 16, 26, 36, 66) is obtained in a straightforward way since these coefficients integrated across the thickness give the stiffness terms. Subsequently, the law of variation of the fibre orientation angle is obtained from the distribution of Q_{ij}.

As the tailoring optimisation of the face plies seeks for optimal stiffness distributions in (α,β), the spatial derivatives of the stiffness coefficients in α,β determine the form of solutions, while the derivatives in ζ are immaterial. On the contrary, the form of solutions is determined by the spatial derivatives in ζ when the core properties are considered, as they are assumed to vary across the thickness.

In this section, terms that appear in the strain component $\varepsilon_{\alpha\alpha}$ and $\varepsilon_{\alpha\zeta}$ are discussed in order to arrive at the solution for $WR_{11}^{\alpha}\ldots WR_{5n}^{\gamma\beta}, WR_{R1}^{\alpha}\ldots WR_{Rn}^{\gamma\beta}$, however the conclusions hold also for $\varepsilon_{\alpha\beta}, \varepsilon_{\beta\beta}$ and $\varepsilon_{\beta\zeta}$, as they have the same mathematical features. A cursory examination of the strains $\varepsilon_{\alpha\alpha}$ and $\varepsilon_{\alpha\zeta}$ reveals that due to the coefficients related to curvatures, the hierarchic terms $(O\zeta^{4}\ldots),(O\zeta^{5}\ldots)$, the coefficients $C_{2\alpha}$, $C_{3\alpha}$, $C_{2\beta}$, $C_{3\beta}$ and b to e and their contributions that appear in the continuity functions $\Phi_{\alpha}^{(k)},\Phi_{\beta}^{(k)},\Psi_{\zeta}^{(k)},\Omega_{\zeta}^{(k)}$, in-plane derivatives of various orders of the functional d.o.f. are involved which determine the form of solutions. Powers of ζ of various orders are also involved, which generate stiffness coefficients that are immaterial for the in-plane optimisation process. For example, this is the case of terms ζ/R_{α} and ζ/R_{β} that appear in the strain definitions and in the expressions of H_{α} and H_{β}.

On the contrary, the derivatives of the displacements explicitly appearing in the strains and those implicitly appearing in the hierarchic terms $(O\zeta^{4}\ldots),(O\zeta^{5}\ldots)$, in the coefficients $C_{2\alpha}$, $C_{3\alpha}$, $C_{2\beta}$, $C_{3\beta}$ and b to e and in the continuity functions $\Phi_{\alpha}^{(k)},\Phi_{\beta}^{(k)},\Psi_{\zeta}^{(k)},\Omega_{\zeta}^{(k)}$ determine the order of differentiation of the stiffness quantities that appear in (16') and (17'). Indeed, once the displacement fields are substituted and the strain energy is computed, the derivatives of the d.o.f. are integrated by parts, resulting into derivatives of the stiffness quantities.

The strain energy given by the transverse shear strain $\varepsilon_{\alpha\zeta}$ is here written in explicit form to show the contributions that are obtained according to the scheme described above. Similar considerations hold also for $\varepsilon_{\alpha\alpha}$ and $\varepsilon_{\beta\zeta}$ as mentioned above. The following expression yields for strain energy due to $\varepsilon_{\alpha\zeta}$

$$\int_\Omega \int_\zeta Q_{44}\left\{\frac{H_\alpha}{H_\zeta}\left\{\left[\left(1+\frac{\zeta}{R_\alpha}\right)u_\alpha^{(0)}-\zeta\frac{u_{\zeta,\alpha}^{(0)}}{A_\alpha}+\zeta(1+(C_{2\alpha}\zeta+C_{3\alpha}\zeta^2))\gamma_\alpha^{(0)}+\right.\right.\right.$$

$$(O\zeta^4\ldots)+\sum_{k=1}^{S}\Phi_\alpha^{(k)}(\zeta-\zeta^{(k)})\mathscr{H}_{.k}\Big]/H_\alpha\Big\}_{,\zeta}+\frac{H_\zeta}{H_\alpha}\Big\{\Big[a+\zeta b+\zeta^2 c+\zeta^3 d+\zeta^4 e+$$

$$\left.\left.\left.(O\zeta^5\ldots)+\sum_{k=1}^{S-1}\Psi_\zeta^{(k)}(\zeta-{}^{(k)}\zeta)\mathscr{H}_k+\sum_{k=1}^{S-1}\Omega_\zeta^{(k)}(\zeta-{}^{(k)}\zeta)^2\mathscr{H}_k\Big]/H_\zeta\Big\}_{,\alpha}\right\}^2 d\Omega d\zeta+\right.$$

$$\int_\Omega \int_\zeta Q_{45}\varepsilon_{\alpha\zeta}\varepsilon_{\beta\zeta}d\Omega d\zeta \tag{18}$$

The contribution of $\varepsilon_{\beta\zeta}$ was left in implicit form for limiting the length of the formula. The derivatives of displacements are converted integrating by parts obtaining the following expressions of the stiffness coefficients

$$\int_\zeta\left\{Q_{44}\left(\frac{H_\alpha}{H_\zeta}\right)\left(1+\frac{\zeta}{R_\alpha}\right)\right\}_{,\zeta}^2 d\zeta;\quad \int_\zeta\left\{Q_{44}\left(\frac{H_\alpha}{H_\zeta}\right)\frac{\zeta}{A_\alpha}\right\}_{,\zeta}^2 d\zeta$$

$$\int_\zeta\left\{Q_{44}\left(\frac{H_\alpha}{H_\zeta}\right)\left(1+\frac{\zeta}{R_\alpha}\right)\frac{\zeta}{A_\alpha}\right\}_{,\zeta} d\zeta \tag{19}$$

Similar expressions are obtained integrating by parts the derivatives of the d.o.f. that appear in the expressions of hierarchic terms and continuity functions written in implicit form in (18) and those due to $\varepsilon_{\beta\zeta}$. The stiffness quantities related to the contribution by $\varepsilon_{\alpha\alpha}$ to the strain energy

$$\int_\Omega \int_\zeta Q_{11}\left\{\frac{1}{H_\alpha}\left[\left(1+\frac{\zeta}{R_\alpha}\right)u_\alpha^{(0)}-\zeta\frac{u_{\zeta,\alpha}^{(0)}}{A_\alpha}+\zeta(1+(C_{2\alpha}\zeta+C_{3\alpha}\zeta^2))\gamma_\alpha^{(0)}+\right.\right.$$

$$(O\zeta^4\ldots)+\sum_{k=1}^{S}\Phi_\alpha^{(k)}(\zeta-\zeta^{(k)})\mathscr{H}_{.k}\Big]_{,\alpha}+\frac{H_{\alpha,\beta}}{H_\alpha H_\beta}\Big\{\left(1+\frac{\zeta}{R_\beta}\right)u_\beta^{(0)}-\zeta\frac{u_{\zeta,\beta}^{(0)}}{A_\beta}+$$

$$\left.\zeta(1+(C_{2\beta}\zeta+C_{3\beta}\zeta^2))\gamma_\beta^{(0)}+(O\zeta^4\ldots)+\sum_{k=1}^{S}\Phi_\beta^{(k)}(\zeta-\zeta^{(k)})\mathscr{H}_{.k}\Big]+\right.$$

$$\frac{H_{\alpha,\zeta}}{H_\alpha H_\zeta}\Big[a+\zeta b+\zeta^2 c+\zeta^3 d+\zeta^4 e+(O\zeta^5\ldots)+(O\zeta^5\ldots)+\sum_{k=1}^{S-1}\Psi_\zeta^{(k)}(\zeta-{}^{(k)}\zeta)\mathscr{H}_k+$$

$$\left.\sum_{k=1}^{S-1}\Omega_\zeta^{(k)}(\zeta-{}^{(k)}\zeta)^2\mathscr{H}_k\right\}^2 d\Omega d\zeta+\int_\Omega \int_\zeta Q_{12}\varepsilon_{\alpha\alpha}\varepsilon_{\beta\beta}d\Omega d\zeta+$$

$$\int_\Omega \int_\zeta Q_{13}\varepsilon_{\alpha\alpha}\varepsilon_{\alpha\beta}d\Omega d\zeta+\int_\Omega \int_\zeta Q_{16}\varepsilon_{\alpha\alpha}\varepsilon_{\zeta\zeta}d\Omega d\zeta \tag{20}$$

are obtained in a similar way as

$$\int_\zeta \left\{ \frac{1}{H_\alpha}\left(1+\frac{\zeta}{R_\alpha}\right) \right\}^2_{,\alpha} d\zeta\,; \quad \int_\zeta \left\{ \frac{1}{H_\alpha}\ \frac{\zeta}{A_\alpha} \right\}^2_{,\alpha} d\zeta;$$

$$\int_\zeta \left\{ \frac{H_{\alpha,\beta}}{H_\alpha H_\beta}\left(1+\frac{\zeta}{R_\beta}\right) \right\}^2 d\zeta\,; \quad \int_\zeta \left\{ \frac{H_{\alpha,\beta}}{H_\alpha H_\beta}\ \frac{\zeta}{A_\beta} \right\}^2 d\zeta;$$

$$\int_\zeta \left\{ \frac{1}{H_\alpha}\left(1+\frac{\zeta}{R_\alpha}\right)\ \frac{1}{H_\alpha}\ \frac{\zeta}{A_\alpha} \right\}_{,\alpha} d\zeta; \quad \int_\zeta \left\{ \frac{1}{H_\alpha}\left(1+\frac{\zeta}{R_\alpha}\right) \right\}_{,\alpha} \frac{H_{\alpha,\beta}}{H_\alpha H_\beta}\left(1+\frac{\zeta}{R_\beta}\right) d\zeta;$$

$$\int_\zeta \left\{ \frac{1}{H_\alpha}\ \frac{\zeta}{A_\alpha} \right\}_{,\alpha} \frac{H_{\alpha,\beta}}{H_\alpha H_\beta}\left(1+\frac{\zeta}{R_\beta}\right) d\zeta; \ \int_\zeta \left\{ \frac{1}{H_\alpha}\ \frac{\zeta}{A_\alpha} \right\}_{,\alpha} \frac{H_{\alpha,\beta}}{H_\alpha H_\beta}\ \frac{\zeta}{A_\beta} d\zeta;$$

$$\int_\zeta \left\{ \left[\frac{H_{\alpha,\beta}}{H_\alpha H_\beta} \right]^2 \left(1+\frac{\zeta}{R_\beta}\right) \frac{\zeta}{A_\beta} \right\} d\zeta \tag{21}$$

along with those due to the implicit terms in (20). It could be noted that in this case either non derived terms, derivatives of the functional d.o.f. across the thickness as well as in-plane derivatives are involved, that play when the stiffness properties of the core or those of faces are optimised, respectively.

Because the radii R_α, R_β can vary from point to point, the solution also depend by their variation. In order to obtain a closed form solution, hereafter it is assumed that they undergo a smooth variation that does not affect the distribution of the stiffness coefficients, or they remain constants like in cylindrical, conical, or spherical shells. If the radii do not exhibit a smooth variation, an approximate solution may be obtained with a numerical scheme.

As the continuity functions involve derivatives of displacements up to the third order, as shown by Icardi and Ferrero (2011), the extremal conditions for the strain energy under variation of the stiffness properties represent a set of partial differential equations up to the fourth order in (α, β) and up to the third order in ζ which should be solved simultaneously. The solutions of the optimization problem of the face plies are represented by exponential functions for elastic coefficients with indices 11, 12, 13, 22, 23, 16, 26, 36, 66, while the terms with indices 44, 45, 55 should be constant, since they involve just first order derivatives of the stiffness properties.

The solutions of the optimization problem of the face plies are represented by exponential functions for elastic coefficients with indices 11, 12, 22, 16, 26 and constant elastic coefficients with indices 44, 45, 55, since just first order derivatives of the stiffness properties with these indices are involved. This is physically consistent with the fact that the transverse shear properties of the plies do not vary with the orientation of the fibres over the plane (α, β). Thus the solution of the extremal problem of the face plies is

$$Q_{ij} = \sum_{m=1}^{n1} [A^{ij}_{1m} e^{(m\alpha + {}^1\varphi^\alpha_n)} + {}^1k_\alpha][A^{ij}_{2i} e^{(m\beta + {}^1\varphi^\beta_n)} + {}^2k_\beta]$$
$$Q_{44} = G;\ Q_{45} = L;\ Q_{55} = M \tag{22}$$

As particular cases, the solution for shells with a constant transverse displacement is represented by trigonometric functions

$$Q_{ij} = \sum_{ki=1}^{n_{ij}} [E_{1k}\sin(k\pi\alpha/L_\alpha + {}^{ij}\varphi_k^\alpha) + {}^{ij}k_\alpha][E_{2k}\sin(k\pi\beta/L_\beta + {}^{ij}\varphi_k^\beta) + {}^{ij}k_\beta]$$
$$Q_{44} = G;\ Q_{45} = L;\ Q_{55} = M \tag{22'}$$

while if shallow shells are further considered it is represented by parabolic functions, like for plates

$$Q_{ij} = [A_1 + A_2\alpha + A_3\alpha^2][B_1 + B_2\beta + B_3\beta]$$
$$Q_{44} = G;\ Q_{45} = L;\ Q_{55} = M \tag{22''}$$

It could be noticed that an exponential solution similar to (22) was found via Fourier transform method in the case of functionally graded materials. The appropriate amplitude, phase, mean value and period in (22) are determined enforcing conditions that make the solution physically consistent (thermodynamic constraint conditions, conservation of energy, Lempriere's and Chentsov's conditions). The stiffness at the bounds of the domain and a convex or a concave shape may also be enforced, since they determine whether the solution minimises or maximises the strain energy components.

As the strain energy due to transverse shears contains non derived terms and derivatives up to the third order in ζ, also the core properties across the thickness should be distributed as exponential functions

$$Q_{ij} = \sum_{m=1}^{n1} A_{1m}^{ij} e^{(m\zeta + {}^1\varphi_n^\zeta)} + A_{2m}^{ij} e^{(-m\zeta + {}^2\varphi_n^\zeta)} + k_\zeta \tag{23}$$

For sandwiches with unsymmetrical properties of faces this distribution holds if ${}^1\varphi_n^\zeta \neq {}^2\varphi_n^\zeta$, $A_{2m}^{ij} \neq A_{2m}^{ij}$. In the next section, the practical implications of variable-stiffness distributions on the response of sandwich shells will be numerically assessed.

4. Numerical results and discussion

A simply-supported, sandwich cylindrical shell in cylindrical bending under sinusoidal loading $p^0\big|^u = P \sin(\pi\beta/\psi)$ is considered in the numerical applications (see Fig. 1). Here α is assumed as the axial straight direction and β as the transverse direction, which traces a circumference of radius R_β. As no variation of occur in α, the only d.o.f. involved are $u_\beta^{(0)}, u_\zeta^{(0)}$, and $u_\beta^{(0)}$. The solution is given as a trigonometric series expansion

$$u_\beta^{(0)} = \sum_{i=1}^{Q1} A^{u\beta}\cos(i\pi\beta/\psi);\quad u_\zeta^{(0)} = \sum_{i=1}^{Q2} A^{u\zeta}\sin(i\pi\beta/\psi);\ \ \gamma_\beta^{(0)} = \sum_{i=1}^{Q3} A^{\gamma\beta}\cos(i\pi\beta/\psi) \tag{24}$$

within the framework of the Galerkin's method. Other sample cases with realistic loading and boundary conditions could be considered, but their solution should be obtained by finite elements. The angle ψ substented by the ends is assumed equal to $\pi/3$, i.e., β traces a circumferential path of length $R_\beta\psi$. The in-plane and transverse displacements and the transverse shear stress are reported in the following normalised form

$$\bar{u}_\beta(\zeta) = \frac{u_\beta(\zeta,0)}{q^0 h};\ \bar{u}_\zeta(\zeta) = \frac{u_\zeta(\zeta,\psi/2)}{q^0 h};\ \bar{\sigma}_{\beta\zeta}(\zeta) = \frac{\sigma_{\beta\zeta}(\zeta,0)}{q^0 S^2 h} \tag{25}$$

The points at $\beta = 0$, or $\beta = \psi/2$ are chosen, since u_β and $\sigma_{\beta\zeta}, u_\zeta$ reach their maximum at these points. To contain the length of the paper, no results are presented for this stress not being equally critical from the viewpoint of damage accumulation, as agreed by the most representative authors. The distributions of the displacements $\bar{u}_\beta, \bar{u}_\zeta$ and of the the transverse shear stress $\bar{\sigma}_{\beta\zeta}$ across the thickness will be reported just for a radius-to-thickness ratio of 4, as this case shows large interfacial stress concentrations, but the effect of optimisation on deflections will be presented also for thin shells.

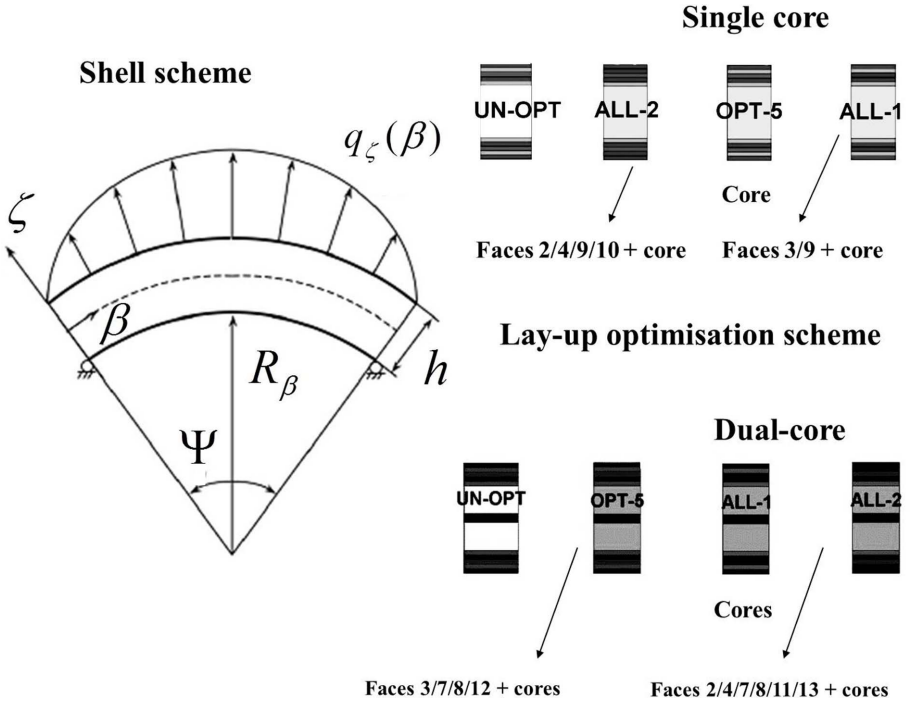

Fig. 1 Scheme of the shell in cylindrical bending, with system of coordinates, loading, boundary conditions and the lay-ups used in this study

Table 1 Properties of the sandwich shell constituting the reference case UN-OPT

	E_1 [Gpa]	E_3 [Gpa]	G_{13} [Gpa]	ν_{13}
MAT 1	1	1	0.2	0.25
MAT 2	33	1	8	0.25
MAT 3	25	1	0.5	0.25
MAT 4	0.05	0.05	0.0217	0.15

MAT 1 to 3 constitute the face layers, MAT 4 is the core. Lay-up $(\text{MAT } 1/2/3/1/3/4)_s$, thickness ratios $(0.010/0.025/0.015/\ 0.020/\ 0.030/0.4)_s$.

Table 2 Mechanical properties of foams used in the optimisation process

	$E_1\ E_2\ E_3$ [Gpa]	$G_{12}\ G_{13}\ G_{23}$ [Gpa]	ν_{23}	ρ [kg/m^3]
ROHACELL	0.140	0.15	0.3	16.3136
AIREX	0.171	0.185/0.430/0.203	0.25	14.8969
VEFER	0.138	0,1027/0.1027/0.6205	0.18	12.4412

The properties of the constituent materials considered in this study are reported in Table 1. The stacking sequence is $(\text{MAT } 1/2/3/1/3/4)_s$ with the following thickness ratios of the constituent layers $(0.010/0.025/0.015/0.020/\ 0.030/0.4)_s$.

4.1 Single core sandwiches

The behaviour of sandwiches with optimised face plies and core is compared to that of the sandwich with uniform core properties and faces with straight-fibre plies, which is referred as UN-OPT. Couples of optimised plies are incorporated according to the scheme of Fig. 1. One increases the bending stiffness at the expense of a moderate increase of transverse shear stresses, the other does the opposite. The core properties are continuously varied within the range of available polymeric foams, i.e., from those of the ROHACELL foam to those of VEFER foam (see Table 2). The stiffer foams are stacked close to the faces, while the weaker ones are stacked at the mid-plane. Low density nanoporous metallic foams with better properties are left to a future study.

4.1.1 Core optimisation

First, just variable core properties are considered, according to Eq. (23). The graded distribution OPT-5 varies from the properties of ROHACELL foam to those of FMNW foams, with the minimum in the thickness middle point. The intermediate distributions OPT-1 to OPT-4 have the same feature, but properties varying from those of the ROHACELL foam to an upper limit that is a progressively increasing fraction of the limit properties of FMNW, here indicated as *max*. OPT-1 corresponds to 5% of *max*, of OPT-2 to 10% of *max*, while OPT-3 and OPT-4 reach 30% and 70% of *max*, respectively. Fig. 2, which give the distributions of $\overline{u}_\zeta, \overline{u}_\beta$ across the thickness for these configurations, shows that the bending stiffness progressively increases from the reference case UN-OPT to the optimised case OPT-5, as $\overline{u}_\zeta$ decreases everywhere across the thickness, while $\overline{u}_\beta$ decreases at the interfaces. As shown by Fig. 3, consequently the transverse shear stress $\overline{\sigma}_{\beta\zeta}$ increases at the interfaces with the core. This appears in antithesis with the aim, but it will be shown that after incorporating optimised plies the interlaminar stress concentrations will decrease, while the bending stiffness will remain the same of the reference case. Fig. 4 shows the results obtained with a step variation of the core properties that approximate the distribution of case OPT-5. It results that this configuration, which may be easily obtained with the current manufacturing techniques, does not results in a significative bending stiffness loss. The transverse shear stress distribution is not reported for containing the length of the paper, but it also does not exhibit relevant variations with respect to the case with continuously variable properties.

Fig. 4 shows also the variation of the bending stiffness that is obtained varying the radius-to-thickness ratio, which is called "*gain*" being expressed as % of the stiffness of the reference configuration UN-OPT. The *gain* is smaller for thick shells but, rapidly increases till to the radius-

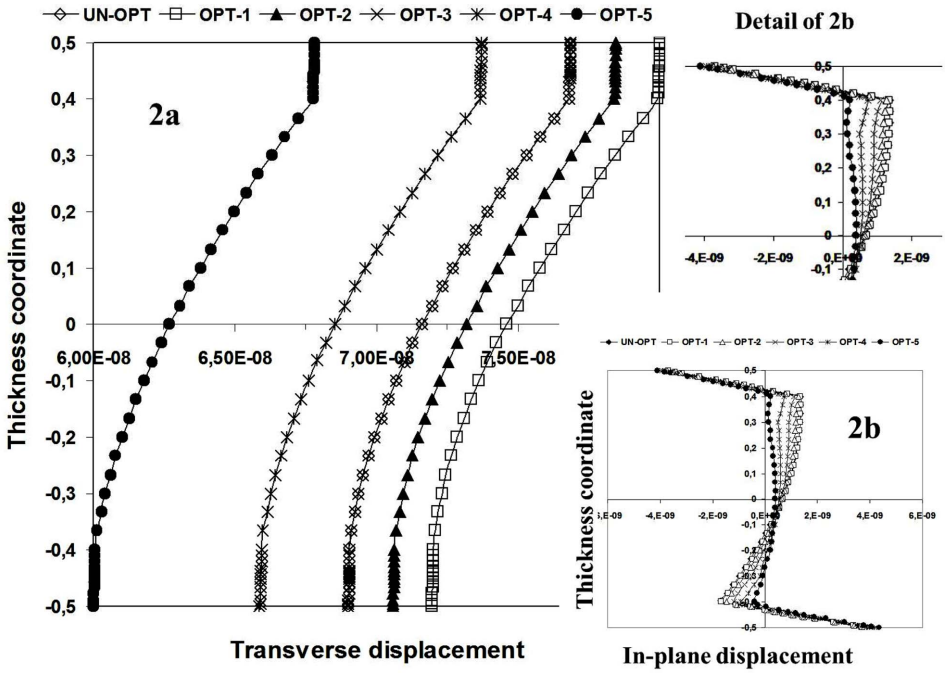

Fig. 2 Transverse and in-plane displacements u_ζ, u_β across the thickness of the sandwich shell with uniform stiffness properties (UN-OPT) and variable core stiffness properties. Properties vary from Rohacel to 5%, 10%, 30%, 70% and 100% of Vefer foam across the thickness (OPT-1 to OPT-5; $R_\beta/h = 4$)

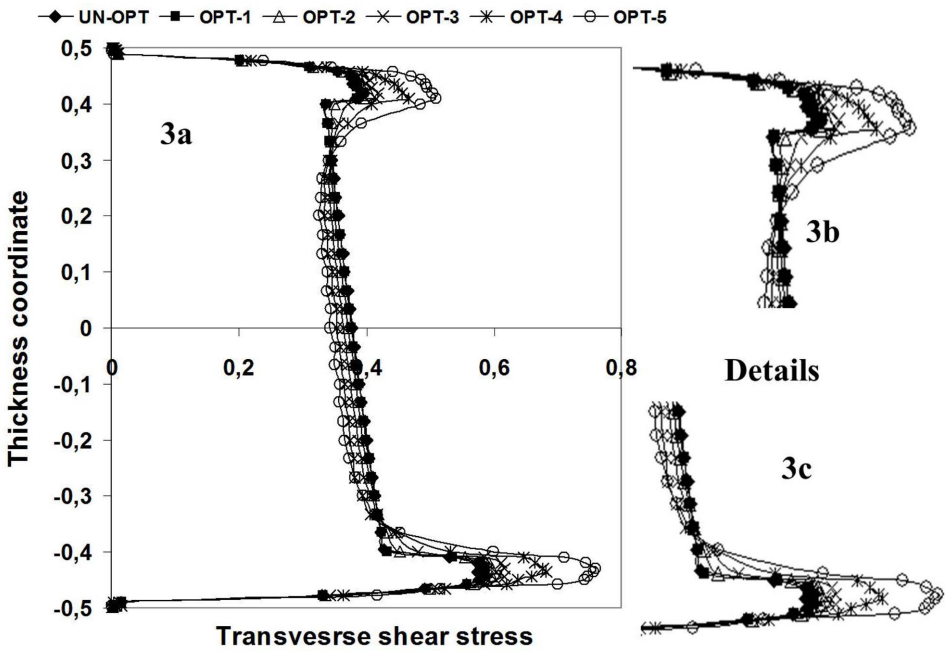

Fig. 3 Through-the-thickness variation of the transverse shear stress $\sigma_{\beta\zeta}$ with uniform core stiffness properties (UN-OPT) and with properties varying from those of Rohacel foam to 5%, 10%, 30%, 70% and 100% of Vefer foam across the thickness, indicated as OPT-1 to OPT-5, respectively ($R_\beta/h = 4$)

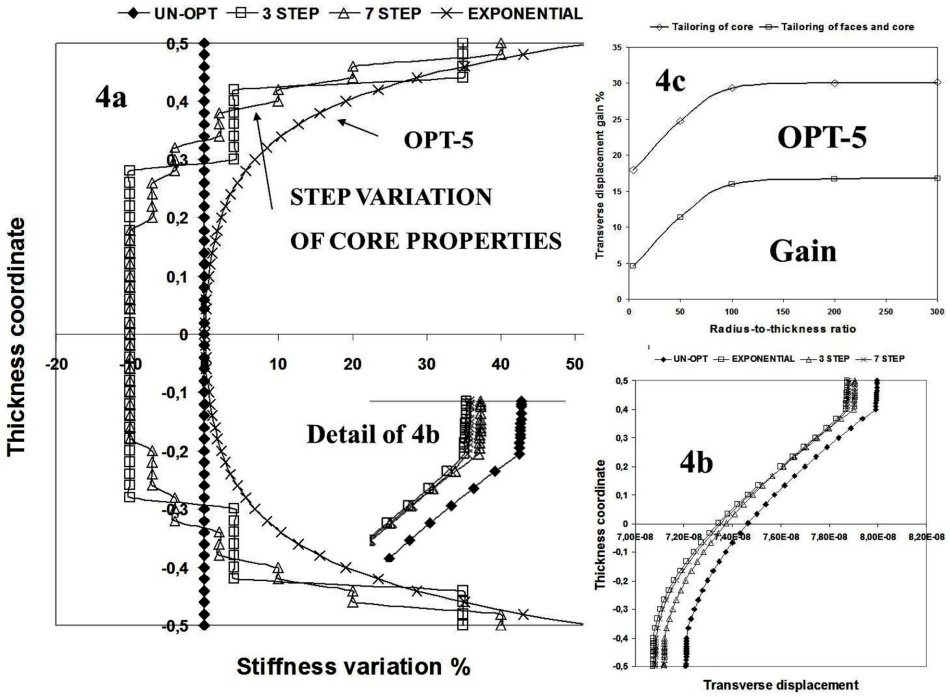

Fig. 4 Transverse displacement u_ζ with exponential OPT-5 and step variation of core properties across the thickness and bending stiffness gain as the ratio of u_ζ by OPT-5 to u_ζ of the uniform stiffness case UN-OPT ($R_\beta/h = 4$)

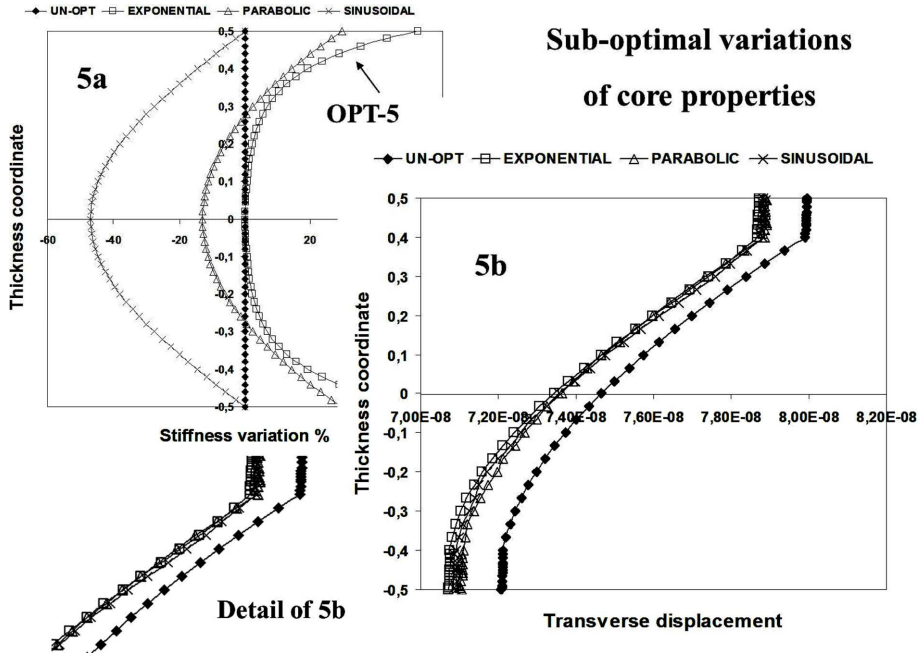

Fig. 5 Transverse displacement u_ζ with suboptimal parabolic and sinusoidal variations of the properties of core across the thickness ($R_\beta/h = 4$)

to-thickness ratio of 100, after which it remains constant.

Thus, in the range of variation of technical interest, the bending stiffness appears to be rather sensitive to the variation of the core properties. In Fig. 4 it is also reported the *gain* for the case with optimised core and faces which is discussed after. It shows a similar behaviour but a lower gain because the goal is keeping the bending stiffness unchanged while recovering the interlaminar stress $\overline{\sigma}_{\beta\zeta}$ at the interfaces. The effects on deflection of sub-optimal parabolic and sinusoidal variations of the core properties reported in Fig. 5 show that sub-optimal graded variations of core properties give results that are equivalent to those of the optimal solution OPT-5. As a step variation of the face properties was also shown to be successful in Icardi and Ferrero (2008), sub-optimal graded or step variation of core and faces properties that approximate the optimal variations OPT-5 can be employed. From the practical viewpoint, this opens the possibility of using simplified distributions that can be easily made with the current manufacturing technologies.

4.1.2 Core and faces optimization

In this case, the core is assumed to have variable properties distributed with the law OPT-5, but also variable-stiffness plies are incorporated in the faces. The 3-rd and the 9-th plies with constant properties are replaced with layers minimising the transverse shear stress in the configuration ALL-1, whereas the 2-nd, 4,9,10-th plies are replaced in ALL-2 with couples of layers minimising bending and transverse shear, respectively. These variable stiffness plies have the properties

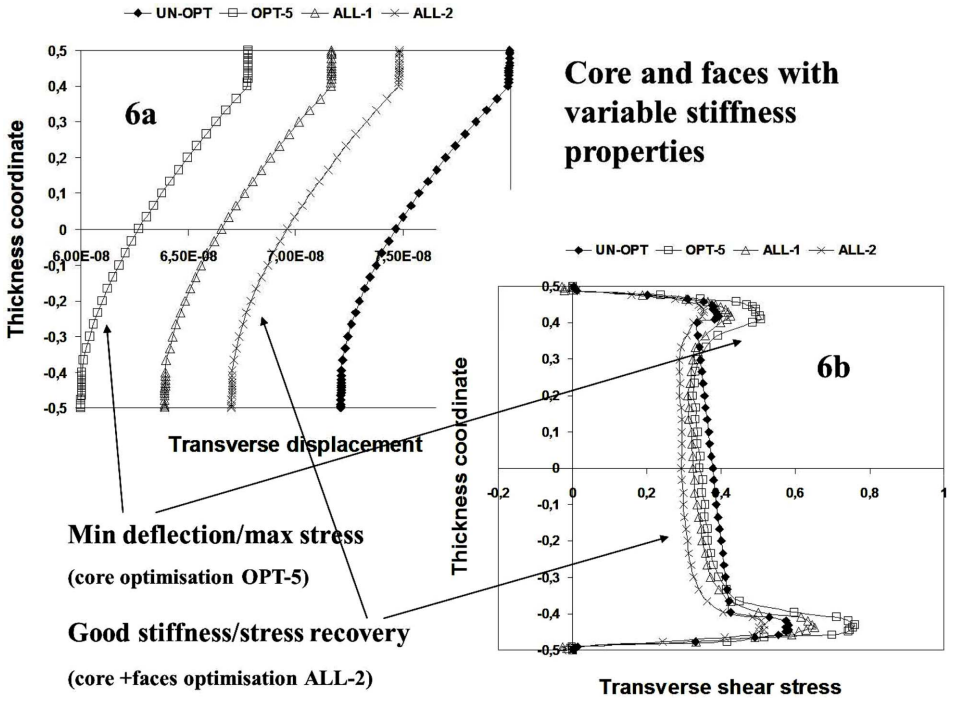

Fig. 6 Transverse displacement u_ζ and shear stress $\sigma_{\beta\zeta}$ with variable stiffness properties of faces and core. Comparison among the reference case UN-OPT, the case with just optimised core OPT-5 and the cases with variable stiffness faces and core. In ALL-1 the 3-rd and the 9-th plies and in ALL-2 the 2-nd, 4,9,10-th plies have variable properties ($R_\beta/h = 4$)

distributed according to Eq. (22) and the coefficients determined choosing the stiffness at the bounds and a concave or convex shape, in order to minimise the energy of transverse shears or that due to bending. Fig. 6 compares the variations of $\overline{u}_\zeta$ and $\overline{\sigma}_{\beta\zeta}$ across the thickness of the reference case with uniform stiffness properties UN-OPT and of the case OPT-5 with optimized core to configurations ALL-1 and ALL-2 with variable core and stiffness faces. The results of Fig. 6 show that the variable stiffness plies reduce the bending stiffness, as also shown by Fig. 4(c), but they recovery the interlaminar stress everywhere across the thickness. Thus the effect of combining OPT-5, which increases the bending stiffness and the interlaminar shear stress in the critical region close to the interfaces, to variable stiffness plies ALL-1, ALL-2 that do the opposite is an improved bending stiffness with lower interlaminar stresses with respect to the reference case UN-OPT. The computations show that the best configuration ALL-2 produce membrane stress $\overline{\sigma}_{\beta\beta}$ in the faces that are up to 20% larger of those of the reference configuration, while the transverse shear stress is decreased by 13% at the interfaces, 12% in the face sheets and 26% close to the interfaces. Applying the 3D version of the Hashin's criterion with *in situ* strengths (criteria are discussed in Icardi, Locatto and Longo 2007), this results in an increase up to 45% of the failure index for tensile/compressive failure of fibres and matrix (strength properties of T300/2500 for the face plies and of ROHACELL for the core), while using the Hou-Petrinic-Ruiz-Hallet's criterion, a consistent decrease of the failure index for delamination up to 45% is shown together with a reduction of the envelope failure index up to 30% considering the combined action of in-plane and out-of-plane stresses in the most critical region close to the interfaces.

4.2 Dual-core sandwiches

Dual-core sandwiches have the capability of bearing loads when failed, as their intermediate face inhibits the deleterious spreading of damage. Though this layer does not contribute to the bending stiffness, the weight is not increased because single-core sandwiches should be over-sized for tolerating damage.

Here the tailoring optimization technique is applied to dual-core sandwiches considering the properties of cores still varying from those of ROHACELL foam, to those of FMNW foams close to the faces and those of faces to vary as in the single-core case. Fig. 7 shows the distributions of $\overline{u}_\beta, \overline{u}_\zeta$ and $\overline{\sigma}_{\beta\zeta}$ across the thickness when the cores have variable-stiffness properties. It is shown that also in this case the displacements $\overline{u}_\beta, \overline{u}_\zeta$ are reduced at the expense of an increase of $\overline{\sigma}_{\beta\zeta}$ at the interfaces. Considering also variable distributions of the face properties, a rather consistent reduction of the transverse shear stresses is achieved with respect to the reference configuration, with an improved bending stiffness, as shown by Fig. 8. The dual-core sandwich spreads the stresses, increasing the strength and the resistance to damage growth since the most relevant interlaminar shear stress concentration take place in the region close to the intermediate face. So, though this face lies on the neutral surface, it bears a relevant part of loading. On the contrary, the single-core sandwich concentrates the shear stress $\overline{\sigma}_{\beta\zeta}$ at the upper and lower interfaces.

The stiffness *gain* increases with increasing the radius-to-thickness ratio up to 100, as for single core sandwiches, but the effect is now much evident. An improved stiffness and reduced interlaminar stresses are easier to obtain than with single-core sandwiches because the presence of an additional face allows to find an advantageous mixture of graded properties. The results of Fig. 8 have been obtained substituting the layers 3,7,8 and 12 in the configuration ALL-1 and the layers 2,4,7,8,11,13 in the configuration ALL-2 with minimum shear layers.

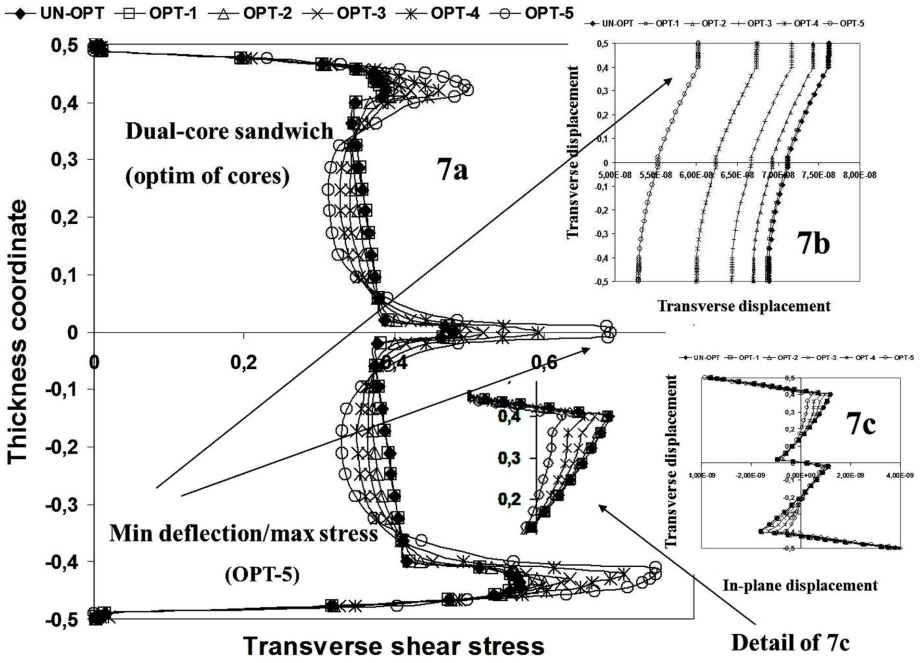

Fig. 7 In-plane displacement u_β, transverse displacement u_ζ and transverse shear stress $\sigma_{\beta\zeta}$ across the thickness of dual-core sandwich with OPT-5 optimised cores. Lay-up properties and thickness of face layers and properties of core are the same of single-core sandwich. Thickness ratio $R_\beta/h = 4$

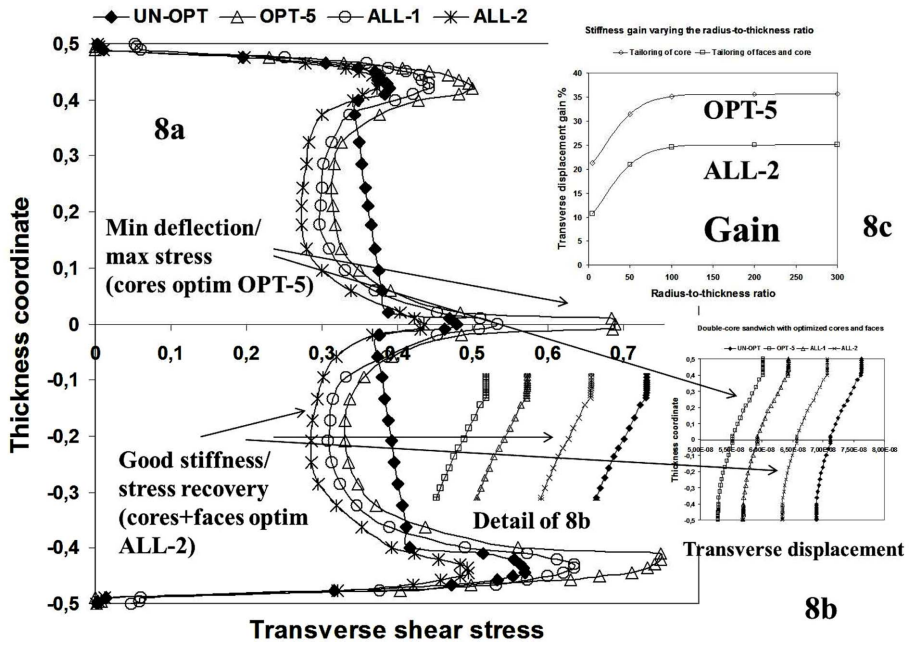

Fig. 8 Transverse displacement u_ζ and shear stress $\sigma_{\beta\zeta}$ across the thickness of dual-core sandwich with optimised cores and faces. Core properties with OPT-5 distributions, face layers with ALL-1 and ALL-2 distributions ($R_\beta/h = 4$)

The membrane stress of the configuration combining OPT5 and ALL-2 is increased with respect to the reference case UN-OPT, while the transverse shear stress is nearly the same at the upper interface, it decreases by 26% across the thickness of the upper core, close to the intermediate face it decreases by 6% and across the lower core and close to the lower face it decreases by 35%. This results in an increase up to 45% of the failure index for tensile/compressive failure of fibres and matrix, as shown by the Hashin's criterion, while as shown by the Hou-Petrinic-Ruiz-Hallet's criterion a reduction of the failure index for delamination up to 78%, is obtained at the interfaces with cores. As a result, the strength to debonding is improved keeping a high bending stiffness.

5. Conclusions

A tailoring optimization technique recently developed by the author has been extended to sandwich shells. The in-plane distribution of the face ply properties and the through-the-thickness distribution of the core properties have been determined by solving the Euler-Lagrange equations of an extremal problem in which the stiffness properties are assumed as the master field. The strain energy due to out-of-plane shear strains and stresses is minimised, while that due to their bending counterparts is maximized.

As shown by the numerical applications to single and dual-core sandwich shells in cylindrical bending, the critical interlaminar stress concentration at the face-core interfaces is consistently reduced from 25 to 35% without any bending stiffness loss.

If just variable stiffness properties of core/cores are considered, the bending stiffness *gain* defined as the ratio to the bending stiffness of the reference case with uniform properties is shown to increase with the radius-to-thickness ratio from 4 up to 100.

Considering variable properties of layers and core/cores, the failure index for tensile/compressive failure of fibres and matrix increases up to 45%, but the failure index for delamination at the face-core interfaces reduces at least by 75%. Hence, the tailoring optimization transfers energy from out-of-plane to in-plane modes. An enhancement of the interfacial bond strength is achieved, which is essential since debonding of the faces from the core/cores, due to the strong coupling between membrane and bending deformations caused by curvature, can lead to a performance loss or a premature failure in service. Suboptimal parabolic, sinusoidal or even step variations of the stiffness properties are shown to achieve nearly the same performance of optimal distributions, thus simplified distributions that can be easily made with the current manufacturing technologies can be successfully employed.

References

Abdalla, M.M., Setoodeh, S. and Gürdal, Z. (2007), "Design of variable stiffness composite panels for maximum fundamental frequency using lamination parameters", *Compos. Struct.*, **8**, 283-291.

Apetre, N.A., Sankar, B.V. and Venkataraman, S. (2002), "Indentation of a sandwich beam with functionally graded core", *Proceedings of 43rd AIAA Structures, Structural Dynamics and Materials Conference*, AIAA paper 2002-1683, Denver, CO, USA.

Apetre, N.A., Sankar, B.V. and Ambur, D.R. (2006), "Low-velocity impact response of sandwich beams with functionally graded core", *Int. J. Solids Struct.*, **43**, 2479-2496.

Apetre, N.A., Sankar, B.V. and Ambur, D.R. (2003), "Functionally-graded sandwich core with arbitrary variation

in properties", *Proceedings of 44th AIAA Structures, Structural Dynamics and Materials Conference*, AIAA paper 2003-1947, Norfolk, VA, USA.
Barth, J. (1990), "Fabrication of complex composite structures using advanced fiber placement technology", *Proceedings of 35th International SAMPE Symposium*, Anaheim, CA, USA, **35**, 710-720.
Chaperon, P., Jones, R., Heller, S., Pitt, F. and Rose, A. (2000), "A methodology for structural optimization with damage tolerance constraints", *Eng. Fail. Anal.*, **7**, 281-300.
Cho, M., Kim, K.O. and Kim, M.H. (1996) "Effcient higher-order shell theory for laminated composites", *Compos. Struct.*, **34**, 197-212.
Diaconu, C.G., Sato, M. and Semine, H. (2002), "Lauyp optimization of symmetrically laminated thick plates for fundamental frequencies using lamination parameters", *Struct. Multidiscip. O.*, **24**, 302-311.
Enders, M. and Hopkins, P. (1991), "Developments in the fiber placement process", *Proceedings of 36th International SAMPE Symposium*, Vol. **36**, San Diego CA, 778-790.
Evans, D. (2001), *Fiber Placement*, Tech. Rep. Cincinnati Machine.
Fuchiyama, T. and Noda, N. (1995), "Analysis of thermal stress in a plate of functionally gradient material", *JSAE Rev.*, **6**, 263-268.
Ghiasi, H., Fayazbakhsh, K., Pasini, D. and Lessard, L. (2010), "Optimum stacking sequence design of composite materials Part II: variable stiffness design", *Compos. Struct.*, **93**, 1-13.
Henao, A., Carrera, M., Miravete, A. and Castejón, L. (2010), "Mechanical performance of through-thickness tufted sandwich strutture", *Compos. Struct.,* **92**, 2052-2059.
Hudson, C.W., Charruthers, J.J. and Robinson, A.M. (2010), "Multiple objective optimisation of composite sandwich structures for rail vehicle floor panels", *Compos. Struct.,* **92**, 2077-2082.
Hyer, M.W. and Charette, R.F. (1991), "Use of curvilinear fiber format in composite structure design", *Proceedings of 30th Structures, Structural Dynamics and Materials Conference, AIAA Mobile,* AL, USA, 2137-2145.
Hyer, M. and Lee, H. (1991), "The use of curvilinear fiber format to improve buckling resistance of composite plates with central circular holes", *Compos. Struct.,* **18**, 239-261.
Kaye, R. and Heller, M. (2000), "Investigation of Shape optimization for the design of life extension options for an F/A-18 airframe FS 470 bulkhead", *J. Strain. Anal.,* **35**, 493-505.
Keller, D. (2010), "Optimization of ply angles in laminated composite structures by a hybrid asynchronous, parallel evolutionary algorithm", *Compos. Struct.,* **92**, 2781-2790.
Icardi, U. (2001), "Higher-order zig-zag model for analysis of thick composite beams with inclusion of transverse normal stress and sublaminates approximations", *Composites: Part B*, **32**, 343-354.
Icardi, U., Locatto, S. and Longo, A. (2007), "Assessment of recent theories for predicting failure of composite laminates", *Appl. Mech. Rev.,* **60**, 76-86.
Icardi, U. and Ferrero, L. (2008), "A new tailoring optimization approach for improving structural response and energy absorption capability of laminated and sandwich composites", *J. Mech. Mater. Struct.*, **3**(4), 729-760.
Icardi, U. and Ferrero, L. (2009a), "Laminated and sandwich panels subject to blast pulse loading", *J. Mech. Mater. Struct.*, **4**(9), 1573-1594.
Icardi, U. and Ferrero, L. (2009b), "Optimisation of sandwich panels with functionally graded core and faces", *Compos. Sci. Technol.*, **69**, 575-585.
Icardi, U. and Ferrero, L. (2010), "Optimisation of sandwich panels to blast pulse loading", *J. Sanswich Struct. Mater.*, **12**(5), 521-550.
Icardi, U. and Ferrero, L. (2011), "Multilayered shell model with variable representation of displacements across the thickness", *Composites: Part B*, **42**, 18-26.
Javirad, D. and Nouri, R. (2011), "A simulated annealing method for design of laminates with required stiffness properties", *Compos. Struct.*, **93**, 1127-1135.
Jegley, D., Tatting, B. and Gürdal, Z. (2005), "Tow-steered panels with holes subjected to compression or shear loading", *Proceedings of AIAA/ASME/ASCE/AHS/ASC 46th Structures, Structural Dynamics and Materials Conference*, Austin, TX, USA, AIAA 2005-2017.
Jones, R., Peng, D., Chaperon, P., Pitt, S., Abramson, D. and Peachey, T. (2000), "Structural optimization with damage tolerant constraints", *Theor. Appl. Fract. Mech.*, **43**, 133-155.
Jung, W.Y.A. (2001), "Combined honeycomb and solid viscoelastic material for structural damping applications",

Proceedings of Thrust Area 2: Seismic Retrofit of Acute Care Facilities, Department of Civil, Structural & Environmental Engineering, University at Buffalo, USA, 41-43.
Krishnapillai, K. and Jones, R. (2009), "Three-dimensional structural design optimization based on fatigue implementing a genetic algorithm and a non-similitude crack growth law", *Finite Elem. Analy. Des.*, **45**, 132-146.
Lakes, R.S. (2002), "High damping composite materials: effect of structural hierarchy", *J. Compos. Mater.*, **36**(3), 287-297.
Li, X.Y. and Liu, D. (1997), "Generalized laminate theories based on double superposition hypothesis", *Int. J. Numer. Meth. Eng.*, **40**, 1197-212.
Liu, J.S. and Hollaway, L. (2000), "Design optimisation of composite panel structures with stiffening ribs under multiple loading cases", *Comput. Struct.*, **78**, 637-647.
Lopes, C.S., Gürdal, Z. and Camanho, P.P. (2008), "Variable-stiffness panels: buckling and first-ply failure improvements over straight-fibre laminates", *Comput. Struct*., **86**, 897-907.
Mahfuz, H., Islam, M.S., Rangari, V.K., Saha, M.C. and Jeelani, S. (2004), "Response of sandwich composites with nanophased cores under flexural loading", *Compos., Part B*, **35**, 543-550.
Martin, J., Langone, R., Pasanen, M. and Mondo, J. (1997), "Cost-effective, automated equipment for advanced composite structure development and production", Tech. Rep., Automated Dynamics Corporation.
Mitra, N. (2010), "A methodology for improving shear performance of marine grade sandwich composites: sandwich composite panel with shear key", *Compos. Struct.,* **92**, 1065-1072.
Narita, Y. and Hodgkinson, J.M. (2005), "Layerwise optimisation for maximising the fundamental frequencies of point-supported rectangular laminated composite plates", *Compos. Struct.*, **69**(2), 127-135.
Pedersen, P. (2003), "A note on design of fiber-nets for maximum stiffness", *J. Elasticity*, **73**(1-3), 127-145.
Reid, R.G. and Paskaramoorthy, R. (2011), "An extension to classical lamination theory for use with functionally graded plates", *Compos. Struct.*, **93**, 639-648.
Sankar, B.V. and Tzeng, J.T. (2002), "Thermal stresses in functionally graded beams", *AIAA J.*, **40**(6), 1228-1232.
Sankar, B.V. (2001), "An elasticity solution for functionally graded beams", *Comput. Sci. Tech.*, **61**, 689-696.
Sivakumar, K., Iyengar, N.G.R. and Kalyanmoy, D. (2000), "Optimization of composite laminates with cutouts using genetic algorithm,variable metric and complex search methods", *Eng. Opt.*, **32**, 635-657.
Sepehri, A., Daneshmand, F. and Jafarpur, K. (2012), "A modified particle swarm approach for multi-objective optimization of laminated composite structures", *Struct. Eng. Mech.*, **42**(3), 335-352.
Setoodeh, S., Abdalla, M.M., Gürdal, Z. and Tatting, B. (2005), "Design of variable-stiffness composite laminates for maximum in-plane stiffness using lamination parameters", *Proceeding of 46th AIAA/ASME/ ASCE/AHS/ASC Struc., Struct. Dynam and Appl. Conf., 13th AIAA/ASME/AHS Adap. Struc. Conf., 7th AIAA Non-Determ Appr. Forum*, 3473-3481.
Suresh, S. and Mortensen, A. (1998), *Fundamentals of Functionally Graded Materials*, IOM Communications Limited, London, UK.
Uys, P.E. and Sankar, B.V. (2003), "Optimal design of a hoist structure frame", *Appl. Math. Model.*, **27**, 963-982.
Venkataraman, S. and Sankar, B.V. (2001), "Analysis of sandwich beams with functionally graded core", *Proceedings of 42nd AIAA Structures, Structural Dynamics and Materials Conference*, AIAA paper 2001-1281, Seattle WA, USA.
Younes, R. and Zaki, W. (2011), "Optimal weaving for 2.5D interlocks", *Compos. Struct.*, **93**, 1255-1264.
Zhu, H. and Sankar, B.V. (2004), "A combined Fourier series-Galerkin method for the analysis of functionally graded beams", *J. Appl. Mech.*, **71**(3), 421-424.
Zhen, W. and Wanji, C. (2008), "A global-local higher order theory for multilayered shells and the analysis of laminated cylindrical shell panels", *Compos. Struct.*, **84**, 350-361.